



1
2
3
4
5
6
7
8
9
10
11
12
13
14
15
16
17
18
19
20
21
22
23
24
25
26
27
28
29
30
31
32

Integrated high-resolution dataset of high intensity Euro-Mediterranean flash floods

William Amponsah^{1,2*}, Pierre-Alain Ayrat^{3,4}, Brice Boudevillain⁵, Christophe Bouvier⁶, Isabelle Braud⁷, Pascal Brunet⁶, Guy Delrieu⁵, Jean-François Didon-Lescot³, Eric Gaume⁸, Laurent Lebouc⁸, Lorenzo Marchi⁹, Francesco Marra¹⁰, Efrat Morin¹⁰, Guillaume Nord⁵, Olivier Payrastré⁸, Davide Zocatelli¹⁰, Marco Borga¹

¹ Department of Land, Environment, Agriculture and Forestry, University of Padova, Legnaro, Italy

² Department of Agricultural and Biosystems Engineering, College of Engineering, KNUST, Kumasi, Ghana

³ ESPACE, UMR7300 CNRS, “Antenne Cevenole”, Université de Nice-Sophia-Antipolis, France

⁴ LGEI, IMT Mines Ales, Univ Montpellier, Ales, France

⁵ Univ. Grenoble Alpes, CNRS, IRD, Grenoble INP, IGE, F-38000 Grenoble, France

⁶ Hydrosociences, UMR5569 CNRS, IRD, Univ. Montpellier, Montpellier, France

⁷ Irstea, UR RiverLy, Lyon-Villeurbanne Center, 68626 Villeurbanne, France

⁸ IFSTTAR, GERS, EE, F-44344 Bouguenais, France

⁹ CNR IRPI, Padova, Italy

¹⁰ Institute of Earth Sciences, Hebrew University of Jerusalem, Israel

*Corresponding author: William Amponsah
Department of Agricultural and Biosystems Engineering, College of
Engineering, KNUST, Kumasi, Ghana
e-mail address: wamponsah@knust.edu.gh
willzamponsah@gmail.com



33 **Abstract**

34 This paper describes an integrated, high-resolution dataset of hydro-meteorological variables (rainfall
35 and discharge) concerning a number of high-intensity flash floods that occurred in Europe and in the
36 Mediterranean region from 1991 to 2015. This type of dataset is rare in the scientific literature because
37 flash floods are typically poorly observed hydrological extremes. Valuable features of the dataset
38 (hereinafter referred to as EuroMedeFF database) include i) its coverage of varied hydro-climatic
39 regions, ranging from Continental Europe through the Mediterranean to Arid climates, ii) the high
40 space-time resolution radar-rainfall estimates, and iii) the dense spatial sampling of the flood response,
41 by observed hydrographs and/or flood peak estimates from post-flood surveys. Flash floods included in
42 the database are selected based on the limited upstream catchment areas (up to 3000 km²), the limited
43 storm durations (up to 2 days), and the unit peak flood magnitude. The EuroMedeFF database
44 comprises 49 events that occurred in France, Israel, Italy, Romania, Germany, and Slovenia, and
45 constitutes a sample of rainfall and flood discharge extremes in different climates. The dataset may be
46 of help to hydrologists as well as other scientific communities because it offers benchmark data for the
47 identification and analysis of the hydro-meteorological causative processes, evaluation of flash flood
48 hydrological models and for hydro-meteorological forecast systems. The dataset also provides a
49 template for the analysis of the space-time variability of flash flood-triggered rainfall fields and of the
50 effects of their estimation on the flood response modelling. The dataset is made available to the public
51 as a "public dataset" with the following DOI: <https://doi.org/10.6096/MISTRALS-HyMeX.1493>.

52

53 *Keywords: flash flood, radar-rainfall estimation, peak discharge estimation, prediction in ungauged*
54 *basins, flood risk management*

55



56 1. Introduction

57 Flash floods are triggered by high-intensity and relatively short duration (up to 1-2 days) rainfall often
58 of spatially confined convective origin (Gaume et al., 2009; Smith and Smith, 2015; Saharia et al.,
59 2017). Due to the relatively small temporal scales, catchment scales impacted by flash floods are
60 generally less than 2000-3000 km² in size (Marchi et al., 2010; Braud et al., 2016). Given the large
61 rainfall rates and the rapid concentration of streamflow promoted by the topographic relief, flash floods
62 often shape the upper tail of the flood frequency distribution of small to medium size catchments.
63 Understanding the hydro-meteorological processes that control flash flooding is therefore important
64 from both scientific and societal perspectives. On one side, elucidating flash flood processes may
65 reveal aspects of flood response that either were unexpected on the basis of less intense rainfall input,
66 or highlight anticipated but previously undocumented characteristics. On the other side, improved
67 understanding of flash floods is required to better forecast these events and manage the relevant risks
68 (Hardy et al, 2016), because knowledge based on the analysis of moderate floods may be questioned
69 when used for forecasting the response to local extreme storms (Collier, 2007; Yatheendradas et al.,
70 2008).

71 However, the relatively reduced small spatial and temporal scales of flash floods, relative to the
72 sampling characteristics of typical hydro-meteorological networks, make these events particularly
73 difficult to monitor and document. In most of the cases, the spatial scales of the events are generally
74 much smaller than the sampling potential offered by even supposedly dense raingauge networks (Borga
75 et al., 2008; Amponsah et al., 2016). Similar considerations apply to streamflow monitoring: often the
76 flood responses are simply ungauged. In the few cases where a stream gauge is in place, streamflow
77 monitoring is affected by major limitations. For instance, peak water levels may exceed the range of
78 available direct discharge measurements in rating curves, causing major uncertainties in the conversion
79 of flood stage data to discharge data. In other cases, stream gauges are damaged or even wiped out by
80 the flood current: in these cases, only part of the hydrograph (usually a segment of the rising limb) is
81 recorded.

82 The call for better observations of flash flood response has stimulated the development of a focused
83 monitoring methodology in the last fifteen years over Europe and the Mediterranean region (Gaume et
84 al, 2004; Marchi et al., 2009; Bouilloud et al., 2009; Calianno et al., 2013; Amponsah et al, 2016). This
85 methodology is built on the use of post-flood surveys, where observations of traces left by water and



86 sediments during a flood are combined with accurate topographic river sections survey to provide
87 spatially detailed estimates of peak discharges along the stream network. However, the important thing
88 to note here is that the survey needs to capture not only the maxima of peak discharges: less intense
89 responses within the flood-impacted region are important as well. These can be contrasted with the
90 corresponding generating rainfall intensities and depths obtained by weather radar re-analysis, thus
91 permitting identification of the catchment properties controlling the rate-limiting processes (Zanon et
92 al., 2010). The large uncertainty affecting indirect peak discharge estimates may be constrained and
93 reduced by comparison with peak discharges obtained from hydrological models fed with rainfall
94 estimates from weather radar and rain gauge data (Amponsah et al., 2016). Post-flood surveys typically
95 start immediately after the event and are carried out in the following weeks and months (Gaume and
96 Borga, 2008), during the so-called Intensive Post-Event Campaigns (IPEC, in the following), before
97 possible obliteration of field evidence from restoration works or subsequent floods.

98 The aim of this paper is to outline the development of the EuroMedeFF dataset, which organises flash
99 flood hydro-meteorological and geographical data from 49 high-intensity flash floods, whose location
100 stretches from the western and central Mediterranean, through the Alps into Continental Europe. The
101 database includes high-resolution radar rainfall estimates, flood hydrographs and/or flood peak
102 estimates through IPEC, and digital terrain models (DTM) of the concerned catchments. The archive
103 provides high-resolution data enabling the analysis of rainfall space-time structure and flood response
104 and the application of hydrological models for the simulation of the flash flood response across varying
105 hydro-climatological contexts. Given the quality and resolution of the rainfall input, the archive
106 provides unprecedented data to examine the impact of space-time resolution in the modelling of high
107 intensity flash floods under different climate and environmental controls. Since results from previous
108 modelling studies are quite mixed, being much of the knowledge either site-specific or expressed
109 qualitatively, the availability of the EuroMedeFF data archive may open new avenues to synthesize this
110 knowledge and transfer it to new situations.

111 This article is organized as follows: the criteria for the EuroMedeFF database development and a
112 summary table of the collected flash floods are presented in Section 2. The methods used to generate
113 the rainfall and discharge datasets are presented in Section 3. Section 4 describes the components of the
114 flash flood datasets, whereas Section 5 discusses the main features of the dataset, based on climatic
115 regions and the two methodologies for discharge data collection (stream gauges and indirect estimates



116 from post-flood analysis). General remarks on the scientific importance of the EuroMedeFF database
117 are provided in the Conclusions section, whereas a link to the freely accessible EuroMedeFF database
118 is provided in the Data Availability section.

119

120 2. Criteria for EuroMedeFF database development

121 The EuroMedeFF database includes data from high intensity flash flood events from different hydro-
122 climatic regions in the Euro-Mediterranean area. To be included in the data set, the following data
123 availability were ensured: i) digital terrain model (DTM) of the impacted region/catchment; ii) weather
124 radar rainfall estimation with high spatial and temporal resolutions, and iii) discharge data from stream
125 gauges and/or post-flood analyses. Rainfall data are provided at a time resolution of 60 min or less and
126 as ‘best available rainfall products’ (i.e., estimates which include the merging of radar and raingauge
127 estimates).

128 Three criteria have been considered for the development of the EuroMedeFF database:

129 *i) Flood magnitude:* A unit peak discharge of $0.5 \text{ m}^3 \text{ s}^{-1} \text{ km}^{-2}$ (this parameter is termed $F_{threshold}$) is
130 considered as the lowest value for defining a flash flood event. This means that, for an event to
131 be included in the database, at least one measured flood peak should exceed the value of
132 $F_{threshold}$. The authors are aware that, depending on climate and catchment size, unit peak
133 discharge of $0.5 \text{ m}^3 \text{ s}^{-1} \text{ km}^{-2}$ can correspond to a severe flash flood (for instance, in the inner
134 sector of the alpine range) or a moderate flash flood (for instance, in many Mediterranean
135 basins). For the sake of simplicity, we adopted the same value of $F_{threshold}$ in all the studied
136 regions. Since the identification of the flash floods included in the database mostly derives from
137 the local observed impact, for most floods the lowest unit peak discharge is much higher than
138 $F_{threshold}$.

139 *ii) Spatial extent:* The upper limit for a catchment impacted by the flood is 3000 km^2 (this
140 parameter is termed $A_{threshold}$). The same meteorological event may have triggered multiple
141 floods (e.g., September and October 2014 floods in France which have affected several
142 mesoscale catchments of about 2000 km^2 - Ardèche, Cèze, Gard and Hérault). In this case, we
143 report several events for the same date, corresponding to different specific catchments with
144 areas less than $A_{threshold}$.

145 *iii) Storm duration:* The upper limit for the duration of the flood-triggering storm is up to 48 hours
146 (this parameter is termed $D_{threshold}$). The rainfall duration is identified by defining a minimum



147 period duration with basin-averaged hourly rainfall intensity less than 1 mm/h over the
148 impacted catchment to separate the time series in consistent events. Here, the minimum
149 duration depends subjectively on hydro-climatic settings and basin size. The reported $D_{threshold}$ is
150 the duration of the rainfall responsible for each event flood peak, separated from other rainfall
151 events that may have occurred before or after the main event depending on the characteristics of
152 the largest involved catchment. In a number of cases in which the features of the flash flood
153 response were specifically affected by wet initial soil moisture conditions, rainfall data is
154 provided for a longer period than the storm duration. This enables to account for antecedent
155 rainfall in the analyses.

156 Given these constraints, the EuroMedeFF database includes 49 high-intensity flash floods: 30 events in
157 France, seven events each in Israel and in Italy, three events in Romania, one event each in Germany
158 and in Slovenia. Table 1 reports summary information of the EuroMedeFF database. In the table, each
159 event is labelled as an ‘*EventID*’, which comprises the impacted catchment/region and the year of
160 occurrence, e.g., ORBIEL1999 (cf. event 1 in Table 1). The ‘*EventID*’ is used in the archive to identify
161 unequivocally the event. For each of the 49 events, the table reports the river basin and the country, the
162 date of the flood peak, the climatic region, the number of river sections for which discharge data are
163 available (both in terms of indirect estimates and streamgauge-based data), with indications of the
164 sections with streamgauge information, the range of basin area for the catchments closed at the studied
165 river sections, the storm duration and the indication of earlier works on the event. In a few cases, more
166 than one flash flood event is reported for the same river basin.

167

168 **3. Rainfall and discharge estimation methods**

169 3.1 Rainfall estimation methods

170 Raw radar data were provided by several sources and elaborated following different procedures
171 depending on the quality and type of available radar and rain gauge data, in order to obtain the best
172 spatially distributed precipitation estimate for each event. In general, original reflectivity in polar
173 coordinates have been used as raw radar data. A set of correction procedures, taking into account the
174 highly non-linear physics of radar detection of precipitation, and procedures for the rain gauge-based
175 adjustment, were used. The procedures include the correction of errors due to antenna pointing, ground
176 echoes, partial beam blockage, beam attenuation in heavy rain, vertical profile of reflectivity and wet



177 radome attenuation, and a two-step bias adjustment that considers the range-dependent bias at yearly
178 scale and the mean field bias at the single event scale. Additional details on the procedures can be
179 found in Bouilloud et al. (2010), Delrieu et al. (2014), Marra et al. (2014), Marra and Morin (2015),
180 Boudevillain et al. (2016) and in the references therein. For French events 7, 26 and 30 in Table 1, only
181 rainfall data from one local rain gauge is available. These floods have been kept in the database
182 because of the interest in including flood response data for very small basins ($< 1\text{km}^2$) and because the
183 small catchment size of the Valescure basin (4km^2) causes the absence of radar rainfall data to be less
184 detrimental than for floods that hit larger catchments.

185

186 3.2 Discharge estimation methods

187 Discharge data in the EuroMedEFF database derive from both streamflow monitoring stations and post-
188 flood indirect estimates of flow peak through IPEC. Streamflow monitoring permits to record flood
189 hydrographs, thus enabling to assess not only discharge but also time response and flood runoff
190 volume. Discharge data from reservoir operations, water levels and use of the continuity equation,
191 when available, share these valuable features with data from stream gauges.

192 Different methods have been used for the indirect reconstruction of flow velocity and peak discharge
193 from flood marks, such as slope-area, slope-conveyance, flow-through-culvert, and lateral super-
194 elevation in bends. Amongst these methods, the most commonly used for the implementation of the
195 dataset presented in this paper is the slope-conveyance, which consists of the application of the
196 Manning-Strickler equation, under assumption of uniform flow, and requires the topographic survey of
197 cross-section geometry and flow energy gradient, computed from the elevation difference between the
198 high water marks along the channel reach surveyed (Gaume and Borga, 2008; Lumbroso and Gaume,
199 2012).

200 Although the identification of river cross-sections suitable for indirect peak discharge assessment has
201 sometimes proved not easy (flood marks can be hardly visible or obliterated by post-flood restoration
202 works), whereas discharge reconstruction in cross sections that underwent major topographic changes
203 is affected by major uncertainties (Amponsah et al., 2016), a wise choice of the cross sections
204 permitted to achieve a spatially-distributed representation of flood response for most studied events.
205 Specific details on the IPEC procedures can be found in the references provided in Table 1.

206



207 4 The EuroMedeFF dataset

208 The EuroMedeFF dataset consists of high-resolution data on rainfall, discharge, and topography. The
209 information in the data archive is categorised into three main groups: *generic*, *spatial* and *discharge*
210 data.

211

212 4.1 Generic data

213 The ‘*Readme*’ text file contains generic data on the date of the flash flood occurrence, the name of the
214 impacted catchment and the Country and Administrative Region of the catchment. Detailed generic
215 information on the spatial data (DTM and radar) and discharge data (flood hydrographs and IPECs) are
216 also elaborated in the ‘*Readme*’ text file. The coordinate systems and grid sizes of the spatial data, and
217 the time resolutions and reference of the radar and flood hydrographs are summarised in the ‘*Readme*’
218 text file.

219

220 4.2 Spatial data

221 *i) Topographic data:* Digital Terrain Model (DTM) with a grid size of 90 m or less but coarse
222 enough to avoid data storage problems. For this reason, we avoided providing DTM data at less
223 than 5 m grid size. For each event, DTM data are provided in compressed ASCII raster files,
224 with label ‘*EventID_DTMXX*’, where *XX* is the grid size in meters. DTM is provided in the
225 local country coordinate system, with a file (*DTMXX_WGS84_LowLeft_corner*) reporting the
226 coordinates of the low-left corner in the WGS84 coordinate system. All the data relative to one
227 country are in the same coordinate system.

228 *ii) Radar-rainfall data:* Corrected and raingauge-adjusted radar-rainfall data are provided with a 1-
229 km or less grid size and temporal resolution appropriate for the flood (typically 60 min or less).
230 For each event, radar data are provided in compressed ASCII raster files, with label ‘*EventID*
231 *_RADAR*’. Radar data are provided, consistent with the DTM data, in the local country
232 coordinate system with a file (*Radar_WGS84_LowLeft_corner*) reporting the coordinates of the
233 low-left corner in the WGS84 coordinate system. At least, all the data relative to one country
234 are in the same coordinate system. The time reference for the radar data is provided as
235 ‘*yymmddHHMM*’.

236



237 4.3 Discharge data

238 *i) Flood hydrographs:* For each event, the location of the available streamgauge stations,
239 upstream area of the basin draining to the station and observed hydrographs are provided in the
240 excel file ‘*EventID_HYDROGRAPHS*’. The coordinates are consistent with the local country
241 coordinate system given for the spatial data, and are also provided in the WGS84 coordinate
242 system. The time reference system for the hydrograph data are consistent with that used for the
243 radar data.

244 *ii) Post-flood data:* Comprehensive data on post-flood surveys through IPEC are provided in the
245 excel file ‘*EventID_IPEC*’. For each section, the location of the surveyed cross-section (outlet),
246 the area of the basin, the indirect estimation method used and peak discharge estimates are
247 provided. When possible, the following further parameters are reported: flood peak time, wet
248 area, slope, roughness parameter, mean flow velocity, Froude number, geomorphic impacts (in
249 three classes – Marchi et al., 2016), and the estimated peak discharge uncertainty range
250 (Amponsah et al., 2016). Coordinates of the surveyed sections are consistent with the local
251 country coordinate system given for the spatial data, and are also provided in the WGS84
252 coordinate system.

253

254 The spatial data (DTM and radar) are provided in ASCII format, compressed to save disk space. The
255 coordinates for radar and DTM data as well as locations of streamgauge and IPEC sections are
256 consistently provided in both local (country-specific) and WGS84 systems. The main advantage of
257 WGS84 is that it avoids possible conversion problems from local coordinate systems, while providing a
258 homogeneous coordinate system throughout the database.

259

260 5 Discussion

261 Figure 1 shows the location of the basins impacted by the flash floods included in the data archive and
262 provides information on the basic features, such as timing of occurrence, size of the largest affected
263 river basin and highest unit peak discharge. The figure shows that the timing of the floods varies
264 gradually from the south-west, where the floods occur mainly in the September to November season, to
265 the east, where the floods occur mainly in the period from autumn to late spring. The shift in
266 seasonality is paralleled by a decreasing basin size and unit peak discharge from south-west to east.
267 These findings are supported by the work of Parajka et al. (2010) who analysed the differences in the



268 long-term regimes of extreme precipitation and floods across the Alpine-Carpathian range, and of
269 Dayan et al. (2015) who analysed the seasonality signal of atmospheric deep convection in the
270 Mediterranean area.

271 We used the Budyko diagram (Budyko, 1974) to characterise the climatic context of the catchments
272 included in the EuroMedeFF database (Figure 2). The Budyko framework plots the evaporation index
273 (i.e., the ratio of mean annual actual evaporation to mean annual precipitation, AET/P) versus the
274 aridity index (i.e., the ratio of mean annual potential evapotranspiration to mean annual precipitation
275 PET/P). The mean values of these variables were calculated for each river basin, so the number of
276 points plotted in Figure 2 is smaller than the total number of flash floods in the database. Figure 2 also
277 reports the empirical Budyko curve (Budyko, 1974), which fits well with the upper envelope of the data
278 included in the data archive. Not surprisingly, the catchments under Arid or Arid-Mediterranean
279 climate display typically water-limited conditions, with the aridity index, $PET/P > 1$. Continental,
280 Alpine and Alpine-Mediterranean catchments lie in the energy-limited sector of the Budyko plot, with
281 aridity index, $PET/P < 1$, indicating wet climate. Mediterranean catchments often display water-limited
282 conditions, although less severe than catchments under Arid and Arid-Mediterranean climate.

283 Overall, 680 peak discharge data are included in the archive: 32% (219) were recorded by river gauging
284 stations and based on data from reservoir operations, and 68% (461) from IPEC surveys. Table 2
285 reports the number of river sections for each of the climatic regions and the corresponding summary
286 statistics of the upstream drainage area. Almost 90% of the included discharge data are from the
287 Mediterranean region, which is consistent with the higher occurrence of high-intensity flash floods in
288 this region compared to other climatic regions in Europe (Gaume et al., 2009; Marchi et al., 2010). The
289 area of the basins included in the archive ranges from 0.27 to 2586 km². Table 2 shows that flash
290 flooding may impact larger basins in the Mediterranean, Alpine and Arid regions than those considered
291 in the Inland Continental region. This support earlier findings from Gaume et al. (2009).

292 Table 3 reports summary statistics of the upstream drainage area for the two discharge assessment
293 methods (stream gauges and indirect methods). As expected, stream gauges correspond to larger areas
294 whereas post-flood surveys play major roles in documenting peak discharges for smaller drainage areas
295 (Borga et al., 2008; Marchi et al., 2010; Amponsah et al., 2016). Nevertheless, the database also
296 includes discharge data from a few measuring stations deployed in small research catchments. This



297 allows to decrease the uncertainty related to the estimation of peak discharge in very small catchments
298 (Braud et al., 2014).

299 The relationship between the unit peak discharge (i.e., peak discharge normalized by the upstream
300 drainage area) and the upstream area was investigated for the EuroMedeFF database to identify the
301 control exerted by catchment size on flood peaks (Figure 3) and to analyse its variation among the main
302 four climatic regions (Figures 4a-d). Not surprisingly, the unit peak discharges exhibit a marked
303 dependence on watershed area. The envelope curve, representing the observed upper limit of the
304 relationship, was empirically derived as a power-law function for all the floods as well as for the four
305 different main climate region. The envelope curve representative for all the floods is similar in shape to
306 that reported by Gaume et al. (2009) and Marchi et al. (2010) in previous analyses in the same hydro-
307 climatic context. However, the multiplier reported here is larger than that reported in earlier analyses,
308 due to the inclusion of recent more intense cases documented in large catchments. Inspection of the
309 multiplier and exponent coefficients of the envelope curves reveals that the same exponent provides a
310 good fit for the different climatic regions, whereas the highest multiplier is reported for the
311 Mediterranean region, with an intermediate value for the Alpine-Mediterranean and Alpine basins, and
312 the same lowest value for Inland Continental, Arid-Mediterranean and Arid basins. For small basin
313 areas (1 to 5 km²), Mediterranean and Alpine catchments are shown to experience similar extreme
314 peaks.

315 Figures 5a-b shows the relationship between unit peak discharge based on the two discharge
316 assessment methods and watershed area in a log-log diagram, together with the envelope curves.
317 Indirect estimates of peak discharges show similar dependence of unit peak discharge on catchment
318 size as that reported in Figure 3, showing that the information content of the overall envelope curve is
319 dominated by the flood obtained based on post flood campaigns. Indeed, peak data from stream
320 gauging stations, show a clearly different exponent of the envelope curve (-0.12) if compared to post-
321 flood indirect peak flow estimates (and to the ones previously shown in Figure 3). The highest values
322 of the peak discharge are often missed by the gauging station because of insufficient density of stream
323 gauge networks and/or damage to the stations during the floods. This sampling problem is more severe
324 in small basins: as a consequence, both the value of the multiplier and the exponent of the envelope
325 equation are lower in Figure 5a than in the plots that include post-flood peak discharge estimation in
326 ungauged streams (Figures 3 and 5b).

327



328 **Conclusions**

329 We presented an observational dataset that provides integrated fine resolution data for high intensity
330 flash floods that occurred in Europe and in the Mediterranean region from 1991 to 2015. The dataset is
331 based on a unique collection of rainfall and discharge data (including data from post-flood surveys) for
332 basins ranging in size from 0.27 to 2586 km². The archive provides high-resolution data enabling a
333 number of flash flood analysis. It allows the analysis of the space-time distribution of causative rainfall,
334 which may be used to investigate methodologies for rainfall downscaling. The data may foster the
335 investigation of the rainfall-runoff relationship at multiple sites within the flash flood environment.
336 This may leads to the identification of possible thresholds in runoff generation which may be related to
337 initial conditions, rainfall rates and accumulations, and catchment properties. Moreover, it allows
338 investigations to clarify the dependence existing between spatial rainfall organisation, basin
339 morphology and runoff response. Finally, the archive may be used as a benchmark for the assessment
340 of hydrological models and flash flood forecasting procedures in various hydro-climatic settings. The
341 availability of fine resolution rainfall data may be used to better understand how rainfall spatial and
342 temporal variability must be considered in hydrological models for accurate prediction of flash flood
343 response. Furthermore, the availability of multiple flash flood response data along the river network
344 may be exploited to better understand how calibration of hydrological models may be transferred
345 across events and sites characterised by different severity.

346 Finally, inspection of the data included in the archive shows the relevance that indirect peak flow
347 estimates have in flash flood analysis, particularly for small basins. This shows the urgency of
348 developing standardised methods for post-flood surveys in order to gather flood response data,
349 including flow types, flood peak magnitude and time, damages, and social response. This is key to
350 further advance understanding of the causative processes and improve assessment of both flash flood
351 hazard and vulnerability aspects (Calianno et al., 2013; Ruin et al., 2014).

352

353 **Data availability**

354 The EuroMedeFF dataset is publicly available and can be downloaded from
355 http://mistrals.sedoo.fr/?editDatsId=1493&datsId=1493&project_name=HyMeX&q=euromedeff. The
356 dataset is also made available with the following unique DOI provided by the HyMeX database
357 administrators: <https://doi.org/10.6096/MISTRALS-HyMeX.1493>.



358

359 **Team list**

360 William Amponsah (WA); Pierre-Alain Ayrat (P-AA); Brice Boudevillain (BB); Christophe Bouvier
361 (CB); Isabelle Braud (IB); Pascal Brunet (PB); Guy Delrieu (GD); Jean-François Didon-Lescot (J-FD-
362 L); Eric Gaume (EG); Laurent Lebouc (LL); Lorenzo Marchi (LM); Francesco Marra (FM); Efrat
363 Morin (EM); Guillaume Nord (GN); Olivier Payrastre (OP); Davide Zoccatelli (DZ) and Marco Borga
364 (MB).

365

366 **Author contributions**

367 Compilation of the flash flood data from Italy, Germany, Slovenia and Romania were done by WA,
368 LM, DZ and MB. The Israeli data were compiled by EM and FM, whereas the French data were
369 compiled by IB and OP, with contributions from P-AA, BB, CB, PB, GD, J-FD-L, EG, LL and GN.
370 The initial draft of the paper was written by WA with the contributions of MB for Sections 1 and 5;
371 EM, FM, LM, IB, OP, GD, EG, DZ and MB for Sections 2 and 4, FM for Section 3.1, and LM for
372 Section 3.2. All authors contributed through their revision of the text.

373

374 **Competing interests**

375 The authors declare that they have no conflict of interest.

376

377 **Acknowledgements**

378 This paper contributes to the HyMeX program (www.hymex.org). Collation of hydrometeorological
379 data and processing of data collated through post flood surveys for the Italian events have been done in
380 the framework of the Next-Data Project (Italian Ministry of University and Research and National
381 Research Council of Italy - CNR). Part of the data was acquired through the Hydrometeorological Data
382 Resources and Technologies for Effective Flash Flood Forecasting (HYDRATE) project (European
383 Commission, Sixth Framework Programme, Contract 037024). Part of the data provided in this data set
384 was acquired during the FloodScale project, funded by the French National Research Agency (ANR)
385 under contract n° ANR 2011 BS56 027. We also benefited from funding by the MISTRALS/HyMeX
386 program (<http://www.mistrals-home.org>), in particular for post-flood surveys. The rainfall reanalysis
387 for the French events were provided by the OHM-CV observatory (observation service supported by



388 the Institut National des Sciences de l'Univers, section Surface et Interfaces Continentales and the
389 Observatoire des Sciences de l'Univers de Grenoble). We thank Arthur Hamburger which work was
390 supported by the Labex OSUG@2020 (Investissements d'avenir – ANR10 LABX56) and the SCHAPI.
391 We also thank SCHAPI, EDF-DTG for providing some of the French stream gauge discharge data, and
392 Meteo France for providing French raingauge and radar input data. For Israel, raw radar data were
393 obtained from E.M.S (Mekorot company), rain gauge data from the Israel Meteorological Service,
394 streamgauge data from the Israel Hydrological Service, and post-flood estimates from reports by the
395 Soil Erosion Research Station at the Ministry of Agriculture and Rural Development. The HyMeX
396 database teams (ESPRI/IPSL and SEDOO/Observatoire Midi-Pyrénées) helped in making the data set
397 available on the HyMeX database.

398

399 References

- 400 Adamovic, M., Branger, F., Braud, I., Kralisch, S., 2016. Development of a data-driven semi-distributed
401 hydrological model for regional scale catchments prone to Mediterranean flash floods. *J. Hydrol.*, 541,
402 Part A: 173-189.
- 403 Amponsah, W., Marchi, L., Zoccatelli, D., Boni, G., Cavalli, M., Comiti, F., Crema, S., Lucia, A., Marra, F.,
404 Borga, M., 2016. Hydrometeorological characterisation of a flash flood associated with major
405 geomorphic effects: Assessment of peak discharge uncertainties and analysis of the runoff response. *J.*
406 *Hydrometeor.*, 17, 3063-3077.
- 407 Borga, M., Boscolo, P., Zanon, F., Sangati, M., 2007. Hydrometeorological Analysis of the 29 August 2003
408 Flash Flood in the Eastern Italian Alps. *J. Hydrometeor.*, 8, 1049–1067.
- 409 Borga, M., Gaume, E., Creutin, J.D., Marchi, L., 2008. Surveying flash flood response: gauging the ungauged
410 extremes., *Hydrol. Processes*, 22, 3883–3885.
- 411 Boudevillain, B., Delrieu, G., Wijbrans, A., Confoland, A., 2016. A high-resolution rainfall re-analysis based on
412 radar–raingauge merging in the Cévennes-Vivarais region, France. *J. Hydrol.*, 541, Part A: 14-23.
- 413 Bouilloud, L., Delrieu, G., Boudevillain, B., Borga, M., Zanon, F. 2009. Radar rainfall estimation for the
414 postevent analysis of a Slovenian flash-flood case: application of the Mountain Reference Technique at
415 Cband frequency. *Hydrol. Earth Syst. Sci.*, 13, 1349–1360.
- 416 Bouilloud, L., Delrieu, G., Boudevillain, B., Kirstetter, P.-E., 2010: Radar rainfall estimation in the context of
417 post-event analysis of flash-flood events. *J. Hydrol.*, 394 (1-2), 17-27.
- 418 Braud, I., and Co-authors, 2014. Multi-scale hydrometeorological observation and modelling for flash flood
419 understanding. *Hydrol. Earth Syst. Sci.*, 18(9): 3733-3761.
- 420 Braud, I., Borga, M., Gourley, J., Hürlimann, M., Zappa, M., Gallart, F., 2016. Flash floods, hydro-geomorphic
421 response and risk management. *J. Hydrol.*, 541: 1-5.
- 422 Brunet, P., Bouvier, C., 2017. Analysis of the September 12th 2015 Lodève (France) flash flood: influence of
423 karsts on flood characteristics, *La Houille Blanche*, n° 3, 2017, p. 39-46.
- 424 Budyko, M.I., 1974. *Climate and Life*. Academic Press, New York.
- 425 Caliano, M., Ruin, I., Gourley, J.J., 2013. Supplementing flash flood reports with impact classifications. *Journal*
426 *of Hydrology*, 477, pp. 1-16.
- 427 Collier, C., 2007. Flash flood forecasting: What are the limits of predictability? *Quarterly Journal of the Royal*
428 *Meteorological Society* 133 (622A), 3–23.
- 429 Dayan, U., Nissen, K., Ulbrich, U., 2015. Review Article: Atmospheric conditions inducing extreme
430 precipitation over the eastern and western Mediterranean. *Natural Hazards and Earth System Sciences*,
431 15 (11), 2525-2544.



- 432 Delrieu, G. and Co-authors, 2005. The catastrophic flash-flood event of 8–9 September 2002 in the Gard region,
433 France: a first case study for the Cévennes-Vivarais Mediterranean Hydro-meteorological Observatory.
434 *J. Hydrometeor.*, 6: 34–52.
- 435 Delrieu, G., Wijbrans, A., Boudevillain, B., Faure, D., Bonnifait, L., Kirstetter, P.-E., 2014. Geostatistical radar-
436 raingauge merging: A novel method for the quantification of rain estimation accuracy. *Advances in*
437 *Water Resources*, 71(0): 110-124.
- 438 Destro, E., Amponsah, W., Nikolopoulos, E.I., Marchi, L., Marra, F., Zoccatelli, D., Borga, M., 2018. Coupled
439 prediction of flash flood response and debris flow occurrence: Application on an alpine extreme flood
440 event. *J. Hydrol.*, 558, 225-237.
- 441 Destro, E., Marchi, L., Amponsah, W., Tarolli, P., Crema, S., Zoccatelli, D., Marra, F., Borga, M., 2016.
442 Hydrological analysis of the flash flood event of August 2, 2014 in a small basin of the Venetian
443 Prealps. *Quaderni di Idronomia Montana*, 34, 307-316 (in Italian, abstract in English).
- 444 Gaume, E., Livet, M., Desbordes, M., Villeneuve, J.P., 2004. Hydrological analysis of the river Aude, France,
445 flash flood on 12 and 13 November 1999. *J. Hydrol.*, 286, 135–154.
- 446 Gaume, E., Borga, M., 2008. Post-flood field investigations in upland catchments after major flash floods:
447 proposal of a methodology and illustrations. *Journal of Flood Risk Management* 1 (4): 175–189.
- 448 Gaume, E.V., and Co-authors, 2009. A collation of data on European flash floods. *J. Hydrol.*, 367, 70–78.
- 449 Greenbaum, N., Margalit, A., Schick, A.P., Sharon, D., Baker, V.R., 1998. A high magnitude storm and flood in
450 a hyperarid catchment, Nahal Zin, Negev Desert, Israel. *Hydrol. Processes*, 12, 1-23.
- 451 Grodek, T., Jacoby, Y., Morin, E., Katz, O., 2012. Effectiveness of exceptional rainstorms on a small
452 Mediterranean basin. *Geomorphology*, 159–160, 156-168.
- 453 Hardy, J., Gourley, J.J., Kirstetter, P.-E., Hong, Y., Kong, F., Flamig, Z.L., 2016. A method for probabilistic
454 flash flood forecasting. *J. Hydrol.*, 541, 480-494.
- 455 Le Bihan, G., Payrastre, O., Gaume, E., Moncoulon, D., and Pons, F.: The challenge of forecasting impacts of
456 flash floods: test of a simplified hydraulic approach and validation based on insurance claim data,
457 *Hydrol. Earth Syst. Sci.*, 21, 5911-5928, <https://doi.org/10.5194/hess-21-5911-2017>, 2017.
- 458 Lange, J., Leibundgut, C., Greenbaum, N., Schick, A. P., 1999. A noncalibrated rainfall-runoff model for large,
459 arid catchments. *Water Resources Research*, 35, 2161-2172.
- 460 Lumbroso, D., Gaume, E., 2012. Reducing the uncertainty in indirect estimates of extreme flash flood
461 discharges. *J. Hydrol.*, 414–415, 16–30.
- 462 Marchi, L., Borga, M., Preciso, E., Gaume, E., 2010. Characterisation of selected extreme flash floods in Europe
463 and implications for flood risk management. *J. Hydrol.*, 394, 118–133.
- 464 Marchi, L., Borga, M., Preciso, E., Sangati, M., Gaume, E., Bain, V., Delrieu, G., Bonnifait, L., Pogačnik, N.,
465 2009. Comprehensive post-event survey of a flash flood in Western Slovenia: observation strategy and
466 lessons learned. *Hydrol. Processes*, 23(26), 3761-3770.
- 467 Marchi, L., Cavalli, M., Amponsah, W., Borga, M., Crema, S., 2016. Upper limits of flash flood stream power in
468 Europe. *Geomorphology*, 272, 68-77.
- 469 Marra, F., Morin, E., 2015. Use of radar QPE for the derivation of Intensity–Duration–Frequency curves in a
470 range of climatic regimes. *J. Hydrolo.*, 531 (2), 427-440.
- 471 Marra, F., Nikolopoulos, E.I., Creutin, J.D., Borga, M., 2014. Radar rainfall estimation for the identification of
472 debris-flow occurrence thresholds. *J. Hydrol.*, 519, 1607-1619.
- 473 Morin, E., Harats, N., Jacoby, Y., Arbel, S., Getker, M., Arazi, A., Grodek, T., Ziv, B., Dayan, U., 2007.
474 Studying the extremes: Hydrometeorological investigation of a flood-causing rainstorm over Israel.
475 *Advances in Geosciences*, 12, 107–114.
- 476 Morin, E., Jacoby, Y., Navon, S., Bet-Halachmi, E., 2009. Towards flash flood prediction in the dry Dead Sea
477 region utilizing radar rainfall information. *Advances in Water Resources*, 32, 1066-1076.
- 478 Naulin J.P., Gaume E., Payrastre O., 2012. Distributed flood forecasting for the management of the road network
479 in the Gard Region (France), *Weather Radar and Hydrology*, IAHS Publication, 351, 544-549.
- 480 Naulin J.P., Payrastre O., Gaume E., 2013. Spatially distributed flood forecasting in flash flood prone areas:
481 Application to road network supervision in Southern France, *Journal of Hydrology*, 486, 88-99,
482 <https://doi.org/10.1016/j.jhydrol.2013.01.044>.



- 483 Niedda M., Amponsah, W., Marchi, L., Zoccatelli, D., Marra, F., Crema, S., Pirastru, M., Marrosu, R., Borgia,
484 M., 2015. The cyclone Cleopatra of November 18, 2013 in Sardinia, event management, measurement
485 and modelling. *Quaderni di Idronomia Montana*, 32/1, 47-58 (in Italian, abstract in English).
- 486 Norbiato, D., Borgia, M., Dinale, R., 2009. Flash flood warning in ungauged basins by use of the Flash Flood
487 Guidance and model-based runoff thresholds. *Meteorological Applications* 16 (1), 65–75.
- 488 Parajka, J., and Co-author, 2010. Seasonal characteristics of flood regimes across the Alpine-Carpathian range. *J.*
489 *Hydrol.*, 394(1-2): 78–89.
- 490 Payrastre, O., Gaume, E., Javelle, P., Janet, B., Fourmigué, P., Lefort, Ph., Martin, A., Boudevillain, B., Brunet,
491 P., Delrieu, G., Marchi, L., Aubert, Y., Dautrey, E., Durand, L., Lang, M., Boissier, L., Douvinet, J.,
492 Martin, C., Ruin, I., 2012. Hydrological analysis of the catastrophic flash flood of 15th June 2010 in the
493 area of Draguignan (Var, France)-TTO2D d’HYMEX, SHF conference “Evénements extrêmes Fluviaux
494 et Maritimes”, Paris, 1-2 février 2012.
- 495 Righini, M., Surian, N., Wohl, E.E., Marchi, L., Comiti, F., Amponsah, W., Borgia, M., 2017. Geomorphic
496 response to an extreme flood in two Mediterranean rivers (northeastern Sardinia, Italy): Analysis of
497 controlling factors. *Geomorphology*, 290, 184-199.
- 498 Rozalis, S., Morin, E., Yair, Y., Price, C., 2010. Flash flood prediction using an uncalibrated hydrological model
499 and radar rainfall data in a Mediterranean watershed under changing hydrological conditions. *J. Hydrol.*,
500 394, 245–255.
- 501 Ruin, I., and Coauthors, 2014. Social and hydrological responses to extreme precipitations: An interdisciplinary
502 strategy for postflood investigation. *Weather, Climate, and Society*, 6, 135-153.
- 503 Ruiz-Villanueva, V., Borgia, M., Zoccatelli, D., Marchi, L., Gaume, E., Ehret, U., 2012. Extreme flood response
504 to short-duration convective rainfall in South-West Germany. *Hydrol. Earth Syst. Sci.*, 16, 1543–1559.
- 505 Saharia, M., Kirstetter, P.-E., Vergara, H., Gourley, J.J., Hong, Y., 2017. Characterization of floods in the United
506 States. *J. Hydrol.*, 548, 524-535.
- 507 Smith, B.K., Smith, J.A., 2015. The flashiest watersheds in the contiguous United States. *J. Hydrometeor.*, 16
508 (6), 2365-2381.
- 509 Tarolli, P., Borgia, M., Morin, E., Delrieu, G., 2012. Analysis of flash flood regimes in the North-Western and
510 South-Eastern Mediterranean regions. *Nat. Hazards Earth Syst. Sci.*, 12, 1255–1265.
- 511 Tramblay, Y., Bouvier, C., Martin, C., Didon-Lescot, J.F., Todorovik, D., Domergue, J.M., 2010. Assessment of
512 initial soil moisture conditions for event-based rainfall–runoff modelling. *J. Hydrol.*, 387, 176–187
- 513 Vannier, O., Anquetin, S., Braud, I., 2016. Investigating the role of geology in the hydrological response of
514 Mediterranean catchments prone to flash-floods: Regional modelling study and process understanding. *J.*
515 *Hydrol.*, 541 (Part A), 158-172.
- 516 Yatheendradas, S., Wagener, T., Gupta, H., Unkrich, C., Goodrich, D., Schaffner, M., Stewart, A., 2008.
517 Understanding uncertainty in distributed flash flood forecasting for semiarid regions. *Water Resources*
518 *Research*, 44 (5), W05S19.
- 519 Zanon, F., Borgia, M., Zoccatelli, D., Marchi, L., Gaume, E., Bonnifait, L., Delrieu, G., 2010. Hydrological
520 analysis of a flash flood across a climatic and geologic gradient: the September 18, 2007 event in
521 Western Slovenia. *J. Hydrol.*, 394, 182–197.
- 522 Zoccatelli, D., Borgia, M., Zanon, F., Antonescu, B., Stancalie, G., 2010. Which rainfall spatial information for
523 flash flood response modelling? A numerical investigation based on data from the Carpathian range,
524 Romania. *J. Hydrol.*, 394, 148–161.
- 525



526 TABLES

527 Table 1. Summary information on the flash flood database

	Event ID	Region/ catchment impacted (Country)	Date of flood peak	Climatic Region	No. of studied watersheds (No. of stream gauges)	Range in Watershed area [km ²]	Storm duration [h]	Previous studies
1	ORBIEL1999	Orbiel (France)	13.11.1999	Mediterranean	21 (1)	2.5 – 239	29	Gaume et al., 2004
2	NIELLE1999	Nielle (France)	13.11.1999	Mediterranean	16 (0)	5 – 125	33	Gaume et al., 2004
3	VERDOUBLE1 999	Verdoble (France)	13.11.1999	Mediterranean	29 (1)	0.35 – 350	30	Gaume et al., 2004
4	VIDOURLE200 2	Vidourle (France)	09.09.2002	Mediterranean	25 (2)	13 – 110	26	Delrieu et al., 2005
5	GARDONS200 2	Gardons (France)	08.09.2002	Mediterranean	66 (6)	1.6 – 1855	25	Delrieu et al., 2005
6	CEZE2002	Ceze (France)	08.09.2002	Mediterranean	12 (4)	7.3 – 1120	25	Delrieu et al., 2005
7	VALESCURE2 006	Valescure (France)	19.10.2006	Mediterranean	4 (4)	0.27 – 3.93	34	Tramblay et al., 2010
8	GARDONS200 8	Gardons (France)	21.10.2008	Mediterranean	33 (9)	0.27 – 1521	21	Naulin et al. , 2012,2013 ; Vannier et al., 2016
9	CEZE2008	Ceze (France)	21.10.2008	Mediterranean	21 (3)	0.95 – 1120	21	Naulin et al. , 2012,2013 ;
10	ARGENS2010	Argens (France)	15.06.2010	Mediterranean	35 (1)	3 – 2550	23	Payrastre et al., 2012 ; Le Bihan et al., 2017
11	ARDECHE2011	Ardeche (France)	3&4.11. 2011	Mediterranean	14 (14)	16 – 2263	31	Adamovic et al., 2016
12	ARDECHE2013	Ardeche (France)	23.10. 2013	Mediterranean	15 (14)	2.2 – 2263	17	
13	ORB2014	Orb (France)	17.09.2014	Mediterranean	7 (3)	3.5 – 335	11	
14	VIDOURLE201 4	Vidourle (France)	18.09.2014	Mediterranean	8 (3)	15 – 770	18	
15	HERAULT2014	Herauld (France)	17.09.2014	Mediterranean	10 (4)	1 – 1305	29	
16	GARDONS201 4-A	Gardons (France)	18& 20.09.2014	Mediterranean	28 (21)	0.27 – 1855	18	



17	ARDECHE2014-A	Ardeche (France)	19.09.2014	Mediterranean	16 (15)	3.4 – 2263	13	
18	ARDECHE2014-B	Ardeche (France)	10&11.10.2014	Mediterranean	17 (15)	3.4 – 2263	41	
19	LEZMOSSON2014	Lez Mosson (France)	07.10.2014	Mediterranean	20 (4)	0.38 – 306	7	
20	GARDONS2014-B	Gardons (France)	10.10.2014	Mediterranean	30 (13)	0.27 – 1855	29	
21	CEZE2014	Ceze (France)	11.10.2014	Mediterranean	6 (3)	77 – 1120	15	
22	ARDECHE2014-C	Ardeche (France)	3&4.11.2014	Mediterranean	16 (16)	3.4 – 2263	15	
23	ARDECHE2014-D	Ardeche (France)	14&15.11.2014	Mediterranean	14 (14)	3.4 – 2263	16	
24	ARDECHE2014-E	Ardeche (France)	27.11.2014	Mediterranean	12 (12)	3.4 – 2263	7	
25	LERGUE2015	Lergue (France)	12.09.2015	Mediterranean	11 (3)	7.5 – 1850	21	Brunet and Bouvier, 2017
26	VALESCURE2015-A	Valescure (France)	12.09.2015	Mediterranean	4 (4)	0.27 – 3.93	26	Tramblay et al., 2010
27	ARGENTIERE2015	Argentiere (France)	03.10.2015	Mediterranean	14 (0)	1.3 – 29	6	
28	BRAGUE2015	Brague (France)	03.10.2015	Mediterranean	16 (0)	0.6 – 41.5	6	
29	FRAYERE2015	Frayere (France)	03.10.2015	Mediterranean	6 (0)	1.3 – 21.4	6	
30	VALESCURE2015-B	Valescure (France)	28.10.2015	Mediterranean	3 (3)	0.27 – 3.93	38	Tramblay et al., 2010
31	ZIN1991	Zin (Israel)	13.10.1991	Arid	1 (1)	233.5	3	Greenbaum et al., 1998; Lange et al., 1999; Tarolli et al., 2012
32	NEQAROT1993	Neqarot (Israel)	23.12.1993	Arid	1 (1)	699.5	4	Tarolli et al., 2012
33	NORTHDEADS EA1994	Teqoa (Israel)	05.11.1994	Arid-Mediterranean	1 (1)	142	4	Tarolli et al., 2012
34	NORTHDEADS EA2001	Darga, Arugot (Israel)	02.05.2001	Arid-Mediterranean	2 (2)	235-70	4	Morin et al., 2009; Tarolli et al., 2012
35	RAMOTMENA SHE2006	Taninim, Qishon (Israel)	02.04.2006	Mediterranean	11 (0)	0.75 – 22	8	Morin et al., 2007; Grodek et al., 2012
36	HAROD2006	Harod (Israel)	27&28.10.2006	Mediterranean	12 (1)	1.2 – 100	5	Rozalis et al., 2010; Tarolli et al., 2012



37	QUMERAN2007	Qumeran (Israel)	12.05.2007	Arid	5 (0)	8.5 – 45.3	3	-
38	STARZEL2008	Starzel (Germany)	02.06.2008	Continental	17 (0)	1 – 119.5	8	Ruiz-Villanueva et al., 2012
39	SORA2007	Selška Sora (Slovenia)	18.09.2007	Alpine-Mediterranean	18 (2)	1.9 – 212	16.5	Zanon et al., 2010
40	FEERNIC2005	Feernic (Romania)	23.08.2005	Continental	1 (1)	168	5.5	Zoccatelli et al., 2010
41	CLIT2006	Clit (Romania)	30.06.2006	Continental	1 (0)	36	4	Zoccatelli et al., 2010
42	GRINTIES2007	Grinties (Romania)	04.08.2007	Continental	1 (0)	52	4	Zoccatelli et al., 2010
43	SEZIA2002	Sesia (Italy)	05.06.2002	Alpine-Mediterranean	6 (6)	75 – 2586	22	
44	FELLA2003	Fella (Italy)	29.08.2003	Alpine-Mediterranean	7 (5)	24 – 623	12	Borga et al., 2007
45	ISARCO2006	Isarco and Passirio (Italy)	3&4.10.2006	Alpine	2 (2)	48 – 75	12.5	Norbiato et al., 2009
46	MAGRA2011	Magra (Italy)	25.10.2011	Mediterranean	36 (3)	0.5 – 936	24	Amponsah et al., 2016
47	VIZZE2012	Vizze (Italy)	04.08.2012	Alpine	3 (1)	45 – 108	18	Destro et al., 2018
48	SARDINIA2013	Cedrino-Posada (Italy)	18.11.2013	Mediterranean	18 (1)	4 – 627	12	Niedda et al., 2015; Righini et al., 2017
49	LIERZA2014	Lierza (Italy)	02.08.2014	Alpine-Mediterranean	8 (0)	1.5 – 12.4	1.5	Destro et al., 2016



529 **Table 2.** Summary statistics for drainage areas for the EuroMedeFF database under different climatic regions

Climatic regions	No. of cases	Mean drainage area [km ²]	Standard deviation	25 th – 75 th quantiles [km ²]
Mediterranean	606	181	417.5	7.5 – 113.7
Alpine and Alpine-Mediterranean	44	150	415.0	8.6 – 97.2
Inland Continental	20	37.6	43.3	2.2 – 48.6
Arid and Arid-Mediterranean	10	148	216.5	13.5 – 210.7

530



531 **Table 3.** Summary statistics for drainage areas for the EuroMedeFF database based on the two classes of
532 discharge assessment (stream gauges vs indirect methods)

Discharge assessment method	No. of cases	Mean drainage area [km ²]	Standard deviation	25 th – 75 th quantiles [km ²]
Stream gauges	219	438	616	60 – 543
Indirect methods (IPECS)	461	49	135	6 – 45

533



534 **FIGURE CAPTION**

535 **Figure 1:** Location of the flash floods in Central and Western Mediterranean, the Alps, and Inland
536 Continental Europe; inset is Eastern Mediterranean (Israel). The length of the arrow represents the area
537 of the largest basin. Colour indicates the magnitude of the largest unit peak discharge. Direction
538 represents the timing of the flash flood occurrence.

539

540 **Figure 2:** Budyko plot for the study basins (P: mean annual precipitation, AET: mean annual actual
541 evapotranspiration, PET: mean annual potential evapotranspiration). In case of multiple nested
542 catchments, only data for the largest one are reported.

543

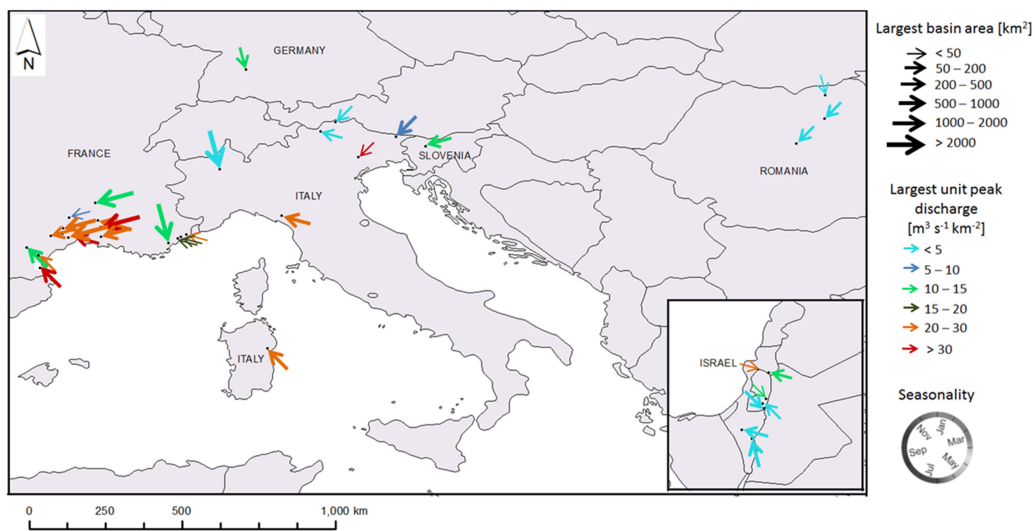
544 **Figure 3:** Unit peak discharges versus drainage areas for the studied flash floods. The envelope curve
545 for upper limit of the relationship is reported.

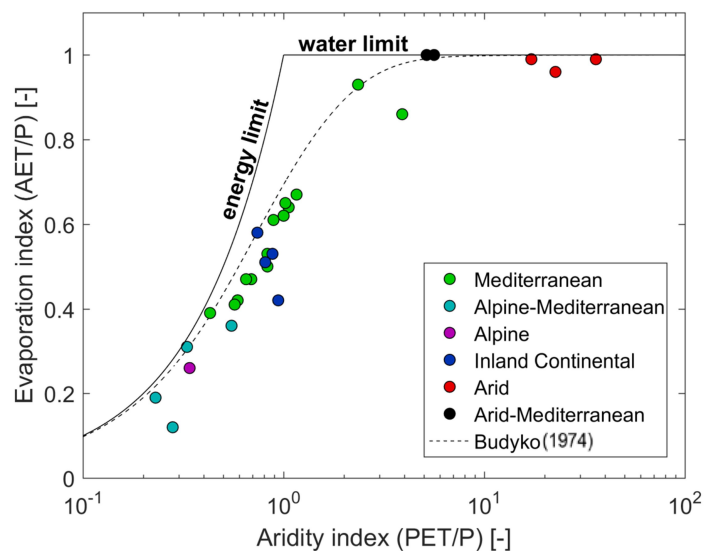
546

547 **Figure 4:** Unit peak discharges versus drainage areas based on climatic regions: (a) Mediterranean
548 catchments, (b) Alpine-Mediterranean and Alpine catchments, (c) Inland Continental, and (d) Arid and
549 Arid-Mediterranean catchments. The envelope curve for each climatic region is reported.

550

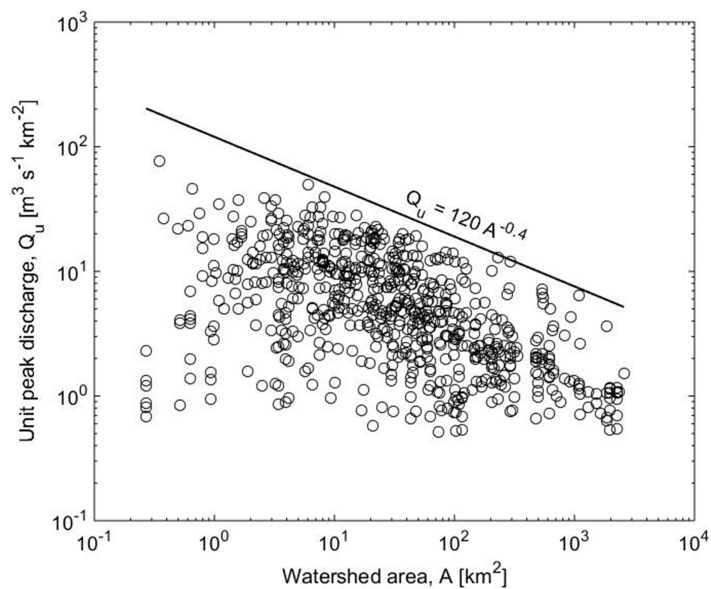
551 **Figure 5:** Unit peak discharges versus drainage areas based on discharge assessment methods: (a)
552 stream gauges and (b) indirect methods. The envelope curves for the upper limits for each method are
553 reported.





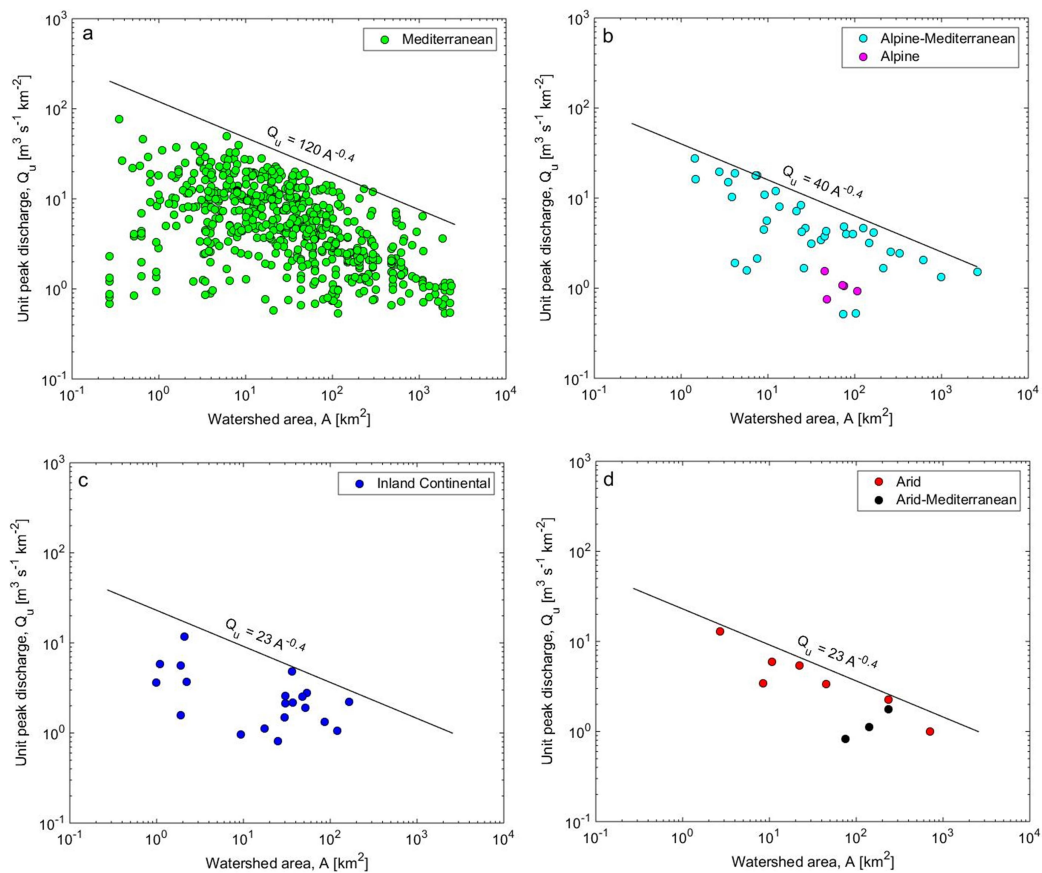
556

557 **Figure 2**



558

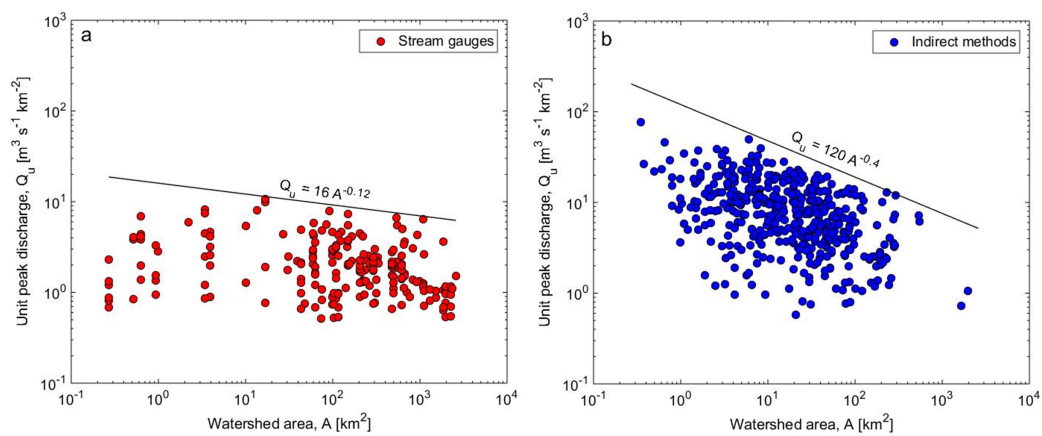
559 **Figure 3**



560

561 **Figure 4**

562



563

564 **Figure 5**